Journal of Colloid and Interface Science 559 (2020) 291–303

Contents lists available at ScienceDirect

Journal of Colloid and Interface Science

journal homepage: www.elsevier.com/locate/jcis

Monovalent – divalent cation competition at the muscovite mica surface: Experiment and theory

Sander J.T. Brugman [a,1], Ben L. Werkhoven [b,1], Eleanor R. Townsend [a], Paolo Accordini [a], René van Roij [b], Elias Vlieg [a,*]

[a] Radboud University, Institute for Molecules and Materials, Heyendaalseweg 135, 6525AJ Nijmegen, the Netherlands
[b] Institute for Theoretical Physics, Center for Extreme Matter and Emergent Phenomena, Utrecht University, Princetonplein 5, 3584 CC Utrecht, the Netherlands

GRAPHICAL ABSTRACT

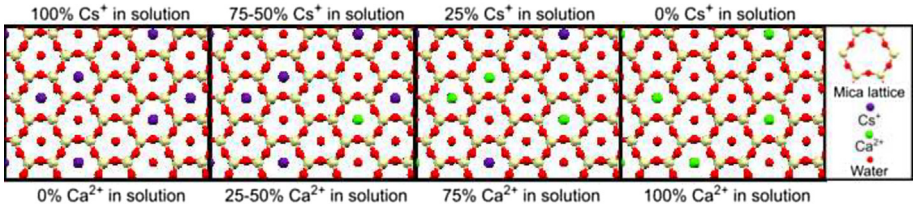

ARTICLE INFO

Article history:
Received 9 August 2019
Revised 2 October 2019
Accepted 3 October 2019
Available online 9 October 2019

Keywords:
Adsorption
Competition
Interface
Surface
Muscovite
Mica
Surface X-ray diffraction
Surface complexation model

ABSTRACT

Hypothesis: Ion adsorption on mineral surfaces depends on several factors, such as the mineral surface structure and the valency, size and hydration of the ion. In order to understand competitive adsorption at mineral surfaces, experimental techniques are required that can probe multiple ionic species at the same time. By comparing adsorption of two different cations, it should be possible to derive the factors governing ion adsorption. Divalent cations are expected to bind stronger to the negatively-charged muscovite surface than monovalent cations.

Experiments: Here, the competition between the monovalent Cs^+ and the divalent Ca^{2+} cation for adsorption at the muscovite mica basal plane was investigated using surface X-ray diffraction. Using an extended surface complexation model, we simultaneously fit the measured cation coverages and net surface charges reported in literature.

Findings: In order to reproduce those complementary data sets, both cation adsorption and anion coadsorption were included in the surface complexation model. Moreover, the intrinsic muscovite surface charge and the maximum of available adsorption sites had to be reduced compared to existing literature values. Competition experiments revealed that the affinity of Cs^+ for the muscovite surface is larger than the affinity of Ca^{2+}, showing that hydration forces are more important than electrostatics.

1. Introduction

The adsorption of cations at mineral surfaces is usually studied under ideal conditions, e.g. by using a single salt, in order to avoid overcomplicating the system. However, in real-world natural environments such as seawater, many different ionic species are present, all competing for the same adsorption sites. A typical example is encountered during low salinity water flooding in enhanced oil recovery. In certain reservoirs, injecting water with low salinity was found to release more initially bound oil molecules than water with high salinity; however, the precise mechanism of this phenomenon is still unknown [1]. One possible

* Corresponding author.
E-mail address: e.vlieg@science.ru.nl (E. Vlieg).
[1] These authors contributed equally to this work.

https://doi.org/10.1016/j.jcis.2019.10.009
0021-9797/

mechanism is the exchange of divalent cations, which bridge polar oil components to the mineral surface, with monovalent cations under low salinity conditions [1,2]. To understand these complex competition processes, experiments that contain multiple ionic species at the same time need to be conducted. However, many frequently-used experimental techniques, such as surface force apparatus (SFA) [3,4] and atomic force microscopy (AFM) [5,6], are not capable of differentiating between cations in a mixture containing multiple salts, due to the 'chemical blindness' of these techniques.

On the other hand, surface X-ray diffraction (SXRD) can be used to investigate a single ion species in an ionic mixture in two ways. If the experimental X-ray energy is close to an absorption edge of one of these ions, anomalous SXRD experiments can be used [7–9]. In these experiments, the element-specific distribution of an ion of interest at the interface can be determined, provided that the X-ray absorption edge energy, at which the element absorbs a photon, is experimentally accessible. A second way to investigate a single ion species in a mixture is by looking at the difference in diffracted intensity, which scales with electron density. A heavy cation will thus have a larger effect on the diffraction pattern than a lighter cation. In a mixture of heavy and light ion species, the electron density will be in between that of only the light cation and only the heavy cation. By using this, it is possible to determine the adsorbed occupancies of both cationic species by using the difference in electron density. In this article, we use the latter method to follow the adsorption of cations at the mineral surface. In this case it is not possible to use anomalous diffraction because the X-ray adsorption edge of the light atom is not experimentally accessible.

Our aim is to identify the relevant mechanisms governing the mineral-electrolyte interface. SXRD, however, is only sensitive to the interfacial structure and does not yield information about the charge of the surface. The surface charge can be obtained by for example zeta potential or AFM measurements [10]. To fully understand the interface, we should ideally combine both the interfacial composition and electrostatic data in a single model. Here we construct a surface complexation model that simultaneously describes both cation coverages measured acquired in this study using SXRD data and electric double layer data previously reported by Bera et al. [11].

Muscovite ideal chemical formula $KAl_2(Si_3Al)O_{10}(OH)_2$) is an excellent mineral model system for this experiment. After cleavage of muscovite, a clean and atomically flat (001) surface is exposed [12]. It is known that this surface is negatively charged due to isomorphous substitution of 25% of Si by Al [13]. The negative charge is compensated by the presence of 0.5 monolayer of K^+ ions. These K^+ ions are located above the center of the six-membered SiO_4 ring, called the cavity site. By submerging muscovite in an electrolyte solution, loosely bound surface K^+ ions can be exchanged by other cations, e.g. Cs^+ or Ca^{2+} [14,15]. Previous research showed that Cs^+ strongly adsorbs to muscovite and significantly changes the diffracted intensity due to its strong X-ray scattering [16–19]. This strong change in diffracted intensity can be used to determine the amount of adsorbed Cs^+ in a solution containing a mixture of Cs^+ and a lighter cation. In this study, Ca^{2+} is chosen as the light cation because of its biological and geophysical relevance (e.g. in seawater and (bio) mineralization). In this way, we can investigate the influence of concentration, valency and hydration energy on the adsorption at the muscovite-electrolyte interface. We will show that we can unite occupancies of adsorbed cations measured with SXRD and electric double layer data measured by AFM in a single surface complexation model. From the analysis of the Cs^+/Ca^{2+} competition, we find that Cs^+ has a higher affinity for the negatively charged muscovite mica surface than Ca^{2+}, despite the lower valency of Cs^+.

2. Experimental and theoretical methods

2.1. Sample preparation

Pieces of muscovite mica (ASTM-V1 quality grade, S&J Trading Inc.) of approximately 45×45 mm^2 were cleaved along the (001) plane using a scalpel and immediately submerged in approximately 50 mL of a salt solution. $CaCl_2$ (Merck, $\geqslant$99.5% pure) and CsCl (Sigma, $\geqslant$98% pure) were used as electrolytes. All measurements were conducted with a total salt concentration of 25 or 475 mM. For at least 30 min, the muscovite remained in solution to equilibrate. During this step, the K^+ surface ions are exchanged for Cs^+ and/or Ca^{2+} ions [14,15]. The concentration of the salts is much higher than that of K^+, which is in the order of μM [19]. Moreover, the individual K^+ ions are expected to reside at the surface for less than a second [20], which is much shorter than the equilibration time of 30 min. After the ion-exchange step, the sample was placed on the sample holder, which was later mounted on the diffractometer. To ensure a stable environment and to prevent evaporation of the liquid film, additional drops of solution were added on top of the sample and in the experimental cell. Subsequently, the sample was covered with Mylar foil (13 μm, Lebow Company) and the excess liquid on top of the muscovite was gently pushed away using a tissue. The pH of the solutions was 6.0 ± 0.6 for all samples, as was measured by a pH meter and pH paper. The surface was scanned to find an area of single surface termination by measuring the (1 1 1.3) reflection [18]. First, the sample was measured at room temperature (RT) and the samples with a total salt concentration of 475 mM were subsequently measured at 63 ± 2 °C (HT). For the HT measurements, the metal sample holder was heated internally using a Lauda heating circulator. This set-up was calibrated in advance to obtain the actual temperature on top of the muscovite crystal. For each experiment, a new piece of muscovite was used.

2.2. Surface X-ray diffraction

Surface X-ray diffraction measurements were performed at the I07 beamline of the Diamond Light Source, using a (2 + 2)-type diffractometer with the crystal mounted horizontally and a Pilatus 100 K area detector. A beam size of 200×100 μm^2 and X-ray energy of 20 keV were selected. For most data sets the (0 0), (1 1), (1 $\bar{1}$), (2 0) and (3 3) crystal truncation rods were acquired, whereas for the pure CsCl and $CaCl_2$ systems additional rods were also obtained. For nonspecular crystal truncation rods, a constant angle of incidence of 0.6° was used. Some rods were measured again after a few hours and did not show any differences, indicating that the X-ray beam does not significantly affect the interface structure. To convert detector images into structure factors, the 'ARTS' MATLAB script was used, whereas the ROD program [21] was used to fit the interfacial structure. Muscovite mica atomic positions and lattice parameters (C2/c, a = 5.1906 Å, b = 9.0080 Å, c = 20.0470 Å, β = 95.757°) were taken from Güven [22]. Anomalous dispersion coefficients at 20 keV [23] and atomic scattering factors [24] were used, taking into account the substitution of 25% of the Si with Al in the bulk crystal structure. Carefully cleaved muscovite mica has only one surface termination, which makes it impossible to use symmetry-equivalent reflections to estimate the error in the data [18]. Systematic errors are typically between 5% and 15%, therefore the error in the data was set to 10% [18]. For some of the data sets an error of 5% was tested, but this did not yield a different interfacial structure compared to an error of 10%. It is important to note that a candidate structure was not judged on the absolute χ^2-value, as this strongly depends on the chosen error. As is common practice, the structure with the lowest

χ^2 and with good agreement with the data points is accepted. In order to increase the relative importance of surface-sensitive regions and to decrease the impact of potential errors close to the Bragg peak, the error in data points close to the Bragg peaks was increased up to 30% [18,19]. Each crystal truncation rod was given an individual scale factor [19]. For the single-salt data sets, the importance of the specular rod was increased by multiplying the weight factor of this crystal truncation rod by a factor of 5.

2.3. Interfacial structure model

The acquired crystal truncation rods were fitted using a similar model as was used for muscovite in contact with a CsI solution [19]. This model consists of the bulk muscovite termination, a cation adsorption site above the muscovite hexagonal cavity with a (partial) hydration shell around it and three water layers. In the upper crystalline layer horizontal and vertical displacements and in-plane and out-of-plane vibration were allowed, whereas the occupancy was set to 100%. At the interface, the occupancy was allowed to vary as well. Other cation adsorption sites were tested as well.

In the interfacial structure model for experiments on mixtures of CsCl and $CaCl_2$, a Cs^+ and a Ca^{2+} adsorption site were incorporated. The position of the Cs^+ and Ca^{2+} ions were fixed to the position found in experiments with only one salt. Both cations keep their hydration water, which results in a hydration structure similar to the single salt conditions. In diffraction experiments, electron densities are probed. The electron density at the cation position is composed of the electron density of Cs^+, Ca^{2+} and water, which does not give unique occupancies for each component. To derive these occupancies, some constraints were added. For all muscovite cavities to be filled, the total occupancy of all cations and water molecules above the muscovite cavity (Θ) should equal 100%, i.e. $\Theta = \theta_{\text{cation}} + \theta_{\text{water}} = 100\%$ for muscovite in contact with a single salt. In the competition experiments, both Cs^+ and Ca^{2+} are present in the solution, so in that case $\Theta = \theta_{Cs^+} + \theta_{Ca^{2+}} + \theta_{\text{water}} = 100\%$. We assume that the ratio between Cs^+ and the water found in the pure Cs^+ experiment, which are both adsorbed at the cavity site, is constant during the competition experiment and that the same holds for the ratio between Ca^{2+} and water at the cavity site. This means the amount of adsorbed water in the cavity site varies systematically, which results in a single fit occupancy for the species above the muscovite cavity.

2.4. Surface complexation model

For the pure CsCl electrolyte, we use a surface complexation model where Cs^+ ions can adsorb above the muscovite cavity and Cl^- ions can coadsorb along with the adsorbed Cs^+. The exact location of the Cl^- ion is not important for this model, as long as it occurs in the Stern layer, see Fig. 1. In the coadsorption model we incorporate the adsorption processes as two chemical reactions

$$\begin{aligned} &S + Cs^+ \rightleftharpoons SCs^+, && K'_{Cs} = \frac{[S][Cs^+]}{[SCs^+]}, \\ &SCs^+ + Cl^- \rightleftharpoons SCsCl, && K'_{CsCl} = \frac{[SCs^+][Cl^+]}{[SCsCl]}, \end{aligned} \tag{1}$$

where S denotes an empty (ion-free) adsorption site (i.e. an empty cavity). We denote the equilibrium adsorption reaction constant of the Cs^+ adsorption reaction by K'_{Cs} and the adsorption reaction constant of the Cl^- coadsorption by K'_{CsCl}. Note that K'_{Cs} and K'_{CsCl} are defined such that these have the dimensions of concentration (in mol/L). The pK value of an adsorption reaction is then defined as $pK \equiv -^{10}\log K'$. We then incorporate these adsorption reactions in the Poisson-Boltzmann formalism [25,26], which combines the Poisson equation for the electrostatic potential, the Boltzmann equation for the density of the ions and global charge neutrality in order to find the distribution of the ions close to a charged surface. The concentration of cations and anions next to a charged surface is altered with respect to the bulk value, which shifts the equilibrium of the adsorption reactions Eq. (1). The shift in the adsorption reaction equilibrium in turn changes the net charge of the surface and thus the density of the dissolved ions close to the surface. The coverage of the surface species can be found using a Langmuir adsorption isotherm which includes this electrostatic feedback mechanism, also known as charge regulation [27]. For the reaction of Eq. (1) the equilibrium condition is given by

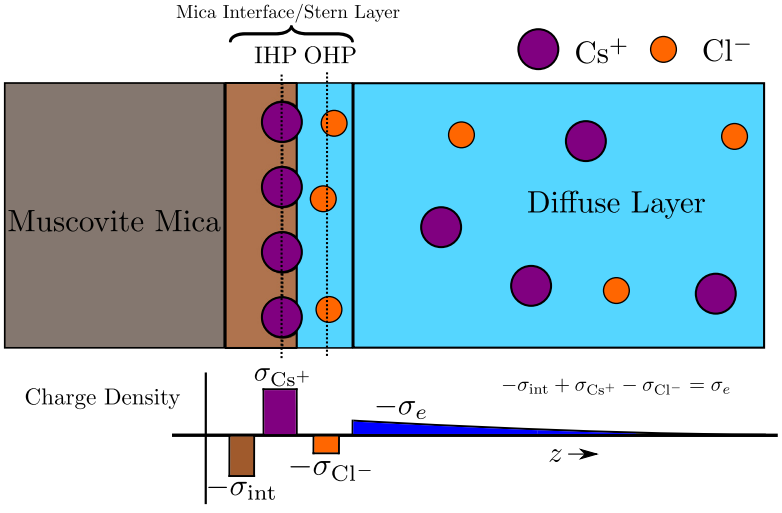

Fig. 1. A schematic representation of the muscovite mica – CsCl electrolyte interface proposed in this article. The interface consists of an interfacial region (brown) where the intrinsic charge of mica σ_{int} is located, an Inner Helmholtz Plane (IHP) where the adsorbed Cs^+ ions are located (density σ_{Cs^+}), an Outer Helmholtz Plane (OHP) with the coadsorbed Cl^- anions (density σ_{Cl^-}) and the diffuse layer. The net surface charge density σ_e is the sum of the intrinsic, Cs^+ and Cl^- contributions. The diffuse layer charge compensates the net surface charge and thus equals $-\sigma_e$, since the system as a whole is charge neutral. The Cs^+ ions in the IHP are confined in all three dimensions, and are therefore measurable with SXRD. The Cl^- ions are confined to the OHP in the direction perpendicular to the surface and are laterally fully disorder and thus, while not visible in non-specular SXRD data, contribute to the surface charge. The ions in the diffuse layer are not confined in any direction. (For interpretation of the references to colour in this figure legend, the reader is referred to the web version of this article.)

$$\theta_{SCs} = \frac{\sigma_{SCs}}{\Gamma} = \frac{\frac{\rho_{Cs} e^{-\phi_0}}{K'_{Cs}}}{1+\frac{\rho_{Cs} e^{-\phi_0}}{K'_{Cs}}+\frac{\rho_{Cs}^2}{K'_{Cs} K'_{CsCl}}},$$
$$\theta_{SCsCl} = \frac{\sigma_{SCsCl}}{\Gamma} = \frac{\frac{\rho_{Cs}^2}{K'_{Cs} K'_{CsCl}}}{1+\frac{\rho_{Cs} e^{-\phi_0}}{K'_{Cs}}+\frac{\rho_{Cs}^2}{K'_{Cs} K'_{CsCl}}}, \quad (2)$$

with $\rho_{Cs} = [Cs^+]$ the bulk Cs^+ concentration, equal to the salinity in the pure CsCl case, Γ the total areal density of adsorption sites, and σ_{SCs} (θ_{SCs}) and σ_{SCsCl} (θ_{SCsCl}) the areal density (occupancy) of the surface groups SCs^+ and SCsCl, respectively. Furthermore, $\phi_0 = e\psi_0/k_BT$, with ψ_0 the electrostatic potential at the surface, e the elementary charge, k_B Boltzmann's constant and T the temperature. In order to keep the number of fit parameters to a minimum, we do not include any Stern-layer capacitances in this model [25,26]. The dimensionless surface potential ϕ_0 is a function of the net charge density $e\sigma_e$ of the surface, or net surface charge density, via the Grahame equation, given, for a 1:1 electrolyte (in SI units), by

$$\phi_0 = 2\,\mathrm{arcsinh}\left(\sqrt{\frac{\pi e^2}{k_B T \epsilon I}}\sigma_e\right), \quad (3)$$

with ϵ the permittivity of water and I the ionic strength ($I = \rho_{Cs} + \rho_{Cl} = 2\rho_{Cs}$ for a 1:1 salt). The net surface charge can be obtained by adding the (negative) intrinsic surface charge of muscovite, $-e\sigma_{int}$, to the positive contribution due to the Cs^+ ions, $e\sigma_{Cs^+} = \sigma_{SCs} + \sigma_{SCsCl}$ and the negative contribution of the Cl^- ions, $-e\sigma_{Cl^-} = -e\sigma_{SCsCl}$, to obtain $e\sigma_e = e\sigma_{SCs} - e\sigma_{int} = e\sigma_{Cs^+} - e\sigma_{Cl^-} - e\sigma_{int}$. The net surface charge density $e\sigma_e$ can be probed by AFM [11], since by charge neutrality the total charge in the diffuse layer must be equal to $-e\sigma_e$. Fig. 1 gives a schematic representation of the muscovite mica - CsCl electrolyte interface, based on the experimental SXRD and AFM data, and the minimal surface complexation model. For a given $\Gamma, K'_{Cs}, K'_{CsCl}$ and salinity ρ_{Cs}, Eqs. (2) and (3) form a closed set that can be solved for the areal densities σ_{Cs} and σ_{CsCl} and surface potential ϕ_0. These equations were solved using the Mathematica software package. The two reaction constants are found by fitting the above described surface complexation model to the SXRD and AFM data. The SXRD data gives the total Cs^+ occupancy, which in our model is equal to the sum of all surface groups that include a Cs^+ ion, i.e. $\theta_{Cs^+} = (\theta_{SCs} + \theta_{SCsCl})$, while the AFM data provides the net surface charge $e\sigma_e$. Therefore, the model gives two distinct parameters that must be predicted correctly before the fit can be accepted.

This model can straightforwardly be extended to include competition with Ca^{2+}. In the case of two cation species, e.g. Cs^+ and Ca^{2+}, the total salinity is equal to the sum of the (bulk) cation concentrations ($[Cs^+]+[Ca^{2+}]$), see the Supporting Information (S1.1) for more details.

3. Results and Discussion

3.1. Interfacial structure

3.1.1. Cs^+-mica interfacial structure

In order to analyse the data on Cs^+/Ca^{2+} competition, we first discuss the structure of the pure systems. To determine the surface structure of muscovite (001) in contact with only CsCl, several crystal truncation rods were acquired for muscovite in contact with 25 mM and 475 mM CsCl. The crystal truncation rods were fitted with a similar model as was used for muscovite in contact with a CsI solution [19]. A good fit was obtained for all data sets (for details we refer to the Supporting Information (S2)).

Fig. 2 shows the electron density according to the interfacial structure model as a function of height for these measurements. The electron density profiles show that Cs^+ adsorbs above the center of the muscovite cavity at a height of 2.16 ± 0.05 Å (Fig. 2a) for both salt concentrations, which is in agreement with literature [16,18,19,28–31]. This peak corresponds to Cs^+ occupancies of $39 \pm 5\%$ and $66 \pm 5\%$ for 25 mM and 475 mM CsCl, respectively, which is in excellent agreement with previous work on CsI [19]. The peak in electron density observed at a height of 4.8 Å above the surface is attributed to the first water layer [19]. All other structural parameters were similar to previous work and are not discussed here, since we focus on the exchange of the cation [19].

3.1.2. Ca^{2+}-mica interfacial structure

Analysis of the measured crystal truncation rods for muscovite mica in contact with pure $CaCl_2$ solutions shows that Ca^{2+} adsorbs above the center of the cavity in an inner-sphere configuration [32]. Contrary to Cs^+, our data for Ca^{2+} indicate different heights at different concentrations: 2.30 ± 0.20 Å at 25 mM and 1.79 ± 0.10 Å at 475 mM (Fig. 2b). These heights correspond to outward displacements with respect to the bulk K^+ position of 0.59 ± 0.20 Å and 0.09 ± 0.10 Å, respectively. Because of the low occupancy of the relatively light Ca^{2+} cation, it is more difficult to pinpoint the exact Ca^{2+} position. At a concentration of 25 mM, there is another peak in electron density visible around 1.6 Å,

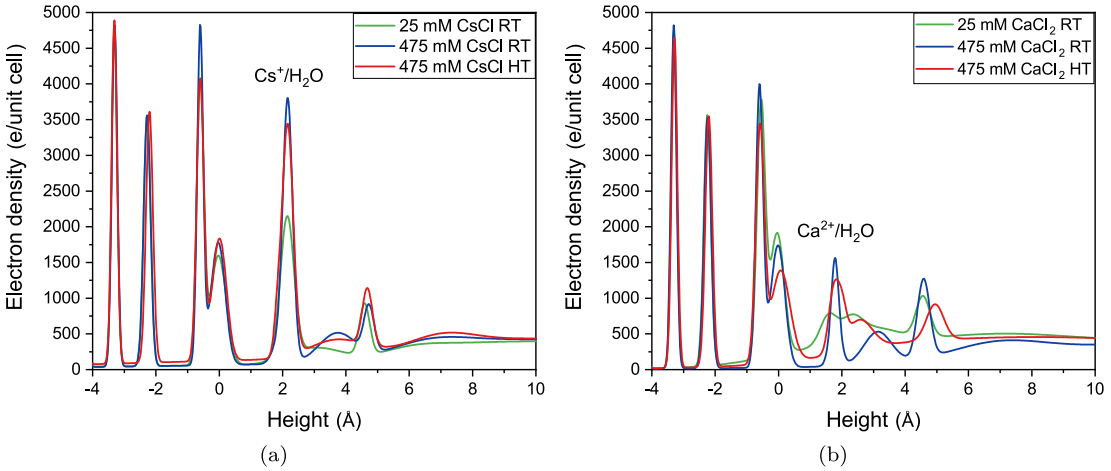

Fig. 2. Laterally averaged electron density perpendicular to the muscovite surface for (a) pure CsCl and (b) pure $CaCl_2$ solutions for salinities 25 mM (green) and 475 mM (blue) at room temperature (RT) and for salinity 475 mM (red) at 63 ± 2 °C (HT). (For interpretation of the references to colour in this figure legend, the reader is referred to the web version of this article.)

which in principle could also correspond to Ca^{2+} adsorption. During the fitting procedure we found that a model with a Ca^{2+} cation at this position gave an inadequate fit. We therefore concluded that this is water located above the cavity. The peaks found for both Ca^{2+} (and Cs^{+}) conditions around 4.6-4.9 Å were attributed to a hydration layer [19]. Besides this layer, two additional water layers complete the interfacial model. All structural parameters for muscovite in contact with Ca^{2+} solutions are summarized in the Supporting Information (S2).

A wide range of values for the height and location of Ca^{2+} have been reported in literature, as shown in Table 1. Schlegel et al. reported a Ca^{2+} height of 2.46 and 2.56 Å using X-ray reflectivity [30]. Loh and Jarvis observed protruding features located above the Si/Al atoms in their AFM images of muscovite mica in contact with a 150 mM $CaCl_2$ solution and attributed this to the adsorption of Ca^{2+} [35]. Molecular Dynamics and Monte Carlo studies showed that Ca^{2+} adsorption is favorable at the negatively charged substitution site, i.e. where Si is substituted by Al [31,33]. To investigate the possibility of this alternative adsorption site, a model in which Ca^{2+} was located above the Si/Al atoms instead of above the cavity was used to fit the measured crystal truncation rods. This significantly lowered the quality of the fit and therefore we reject this alternative adsorption site. Also a model involving both adsorption sites did not improve the fit. The difference between the adsorption height we find here and that reported in literature might also be a consequence of the X-ray diffraction measurements, which are sensitive to spatially ordered parts of the interface. If indeed Ca^{2+} has multiple adsorption states, SXRD might be more sensitive to the most ordered adsorption state, i.e. the adsorption site above the muscovite cavity which is closer to the surface than the adsorption site above the Si/Al atoms [31].

For divalent cations we expect half the occupancy of monovalent cations in order to compensate for the negative muscovite surface charge. Sr^{2+} and Ba^{2+} occupancies close to the expected 25% were previously reported for muscovite in contact with 10 mM $SrCl_2$ and $BaCl_2$ solutions [36]. The best fit of our measured crystal truncation rods for muscovite in contact with 25 mM $CaCl_2$ is obtained for a Ca^{2+} occupancy of 28 ± 8%, which is within the accuracy the same as the reported Sr^{2+} and Ba^{2+} occupancies. However, for high $CaCl_2$ concentrations, the Ca^{2+} occupancy increases to 45 ± 8%. This suggests an excess surface charge of approximately +1.7 e/nm^2, which is too high to compensate for in the diffuse layer [37,11] and strongly suggests anion coadsorption. This can possibly explain the lower Ca^{2+} height found at high salinity. Although there is no direct evidence of well-ordered anion coadsorption on monovalent cations [19,38], there is some evidence for the formation of $CaCl^{+}$ ion pairs. In an X-ray photoelectron spectroscopy study Xu and Salmeron found that Cl^{-} could not be washed away fully from the Ca^{2+}-mica surface [39]. Furthermore, the coadsorption of Cl^{-} to Ca^{2+} has been suggested before on montmorillonite [40] and gibbsite [41]. Our current data, however, does not provide enough information on the position and occupancy of the anion.

3.1.3. Trends in cation height

Previously, using SXRD the adsorption height on muscovite mica was found to increase with the ionic radius for monovalent Rb^{+} and Cs^{+} [18]. A similar trend was observed for divalent Sr^{2+} and Ba^{2+} [36]. This is summarized in Fig. 3a, which shows the

Table 1
Height of cations adsorbed to muscovite mica at room temperature. The average bulk position of the topmost oxygen atoms of the muscovite structure is defined as 0 in the z-direction.

Study	Technique	Solute	Concentration (mM)	Cation height (Å)	Position cation
This study	SXRD	$CaCl_2$	25	2.30 ± 0.20 Å	Cavity
This study	SXRD	$CaCl_2$	475	1.79 ± 0.10 Å	Cavity
Schlegel et al. [30]	X-ray reflectivity	$CaCl_2$	10	2.46	–
Schlegel et al. [30]	X-ray reflectivity	$CaCl_2$	500	2.56	–
Kobayashi et al. [31]	Molecular dynamics	Ca^{2+}	–	1.49	Cavity
Kobayashi et al. [31]	Molecular dynamics	Ca^{2+}	–	2.65	Si/Al substitution
Meleshyn [33]	Monte Carlo	Ca^{2+}	–	1.53–1.72	Si/Al substitution
Adapa et al. [34]	Monte Carlo	Ca^{2+}	–	2.23 & 2.50	Multiple states

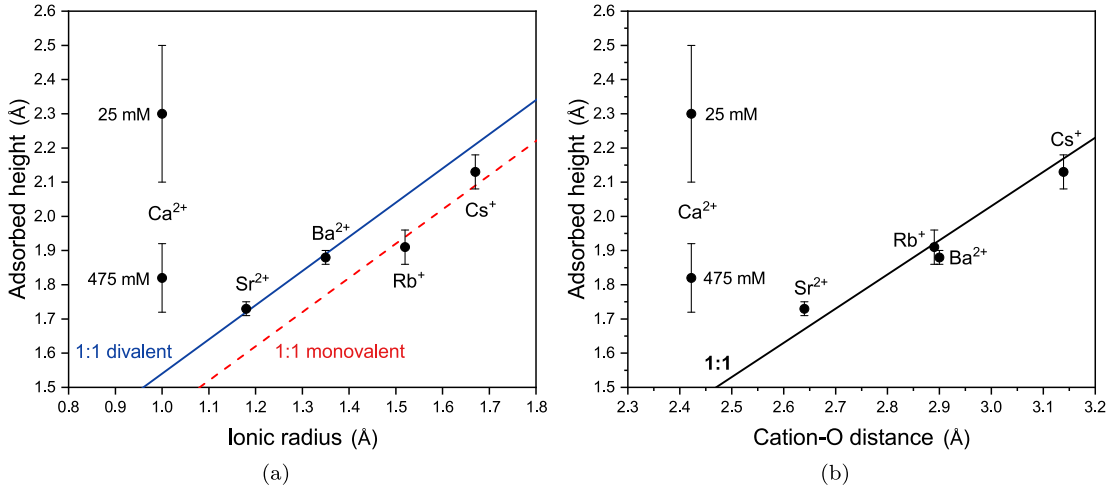

Fig. 3. Adsorbed height of cations determined using SXRD as function of (a) the unhydrated ionic radius [42] and (b) the distance between the cation and the O atom of the first hydration shell [43]. The adsorption height was measured at a cation concentration of 11 mM for Rb^{+} and 10 mM for both Sr^{2+} and Ba^{2+} [18,36]. The Cs^{+} adsorption height was found to be independent of concentration between 2 and 1000 mM [19]. The 1:1 monovalent (red, dashed) and 1:1 divalent lines (blue, solid) in (a) and the 1:1 line (black, solid) in (b) indicate the trend for heavier elements. (For interpretation of the references to colour in this figure legend, the reader is referred to the web version of this article.)

adsorbed height as function of the unhydrated ionic radius. Interestingly, Ca^{2+} clearly does not follow the divalent trend, neither for high nor for low salt concentrations. The Ca^{2+} ion is significantly smaller than the other divalent cations and could be expected to adsorb at a height of approximately 1.54 Å above the surface, according to the trend. The deviation from the trend might be caused by the strong hydration shell of Ca^{2+}. The SXRD interfacial structure shows that there is no water underneath the Ca^{2+} ion and thus that Ca^{2+} is only partially hydrated. Since the hydration energy of Ca^{2+} is relatively high, and the ionic radius relatively small, it is more favourable for Ca^{2+} to adsorb at a height larger than based purely on its ionic radius, since then Ca^{2+} is able to retain more water molecules in its hydration shell. In Fig. 3b, the adsorbed height as function of the distance between the cation and O atom of the first hydration shell is shown. Here, a approximate 1:1 relationship is found for all cations, except for Ca^{2+}. This once more shows the effect of the strong hydration of Ca^{2+}.

3.1.4. Effect of temperature

All measurements considered so far were performed at room temperature. The measurements at high temperature (HT) were performed at 63 ± 2 °C and showed that the Cs^+ occupancy at a CsCl concentration of 475 mM remains constant within the error bars ($67 \pm 5\%$) compared to room temperature ($66 \pm 5\%$). Moreover, the cation remains located at the same height (2.16 ± 0.05 Å, see Fig. 2a). Similar to Cs^+, no significant changes in surface structure are observed for Ca^{2+} at high temperature when compared to the room temperature structure. At high temperature, Ca^{2+} is found to adsorb with an occupancy of $47 \pm 8\%$ at a height of 1.74 ± 0.10 Å (Fig. 2b), compared to an occupancy of $45 \pm 8\%$ at a height of 1.79 ± 0.10 Å for the same concentration at room temperature.

3.2. Development of the surface complexation model

In order to understand the competition between Cs^+ and Ca^{2+}, we first develop the surface complexation model using both SXRD and surface charge data on the single ion data already available for Cs^+. The Cs^+ adsorption isotherm (Fig. 4a) shows the Cs^+ occupancy as a function of salinity for previously reported data for CsCl (in green) [18] and CsI (in black) [19] as well as occupancies of CsCl of the current work (in red), which are in excellent agreement with each other. Together with the net surface charge as measured by Bera et al. (Fig. 4b) [11], the Cs^+ occupancies are used to develop the surface complexation model. The adsorption isotherm does have the typical 'S-curve' shape, with a transition from a low coverage plateau (approximately 35%) at low salinity to a high coverage plateau (approximately 65%) at high salinity. A muscovite surface without any adsorbed ions has an intrinsic negative surface charge of 1*e* per unit cell, which can be exactly compensated by a monovalent cation occupancy of 50% (dashed line in Fig. 4a). Fig. 4b, however, shows that the net surface charge of the muscovite-electrolyte interface does not exceed -0.1 e/nm^2, corresponding to approximately 3% of the total number of adsorption sites. The Cs^+ coverage data thus shows that Cs^+ alone does not compensate the intrinsic surface charge; below approximately 10 mM the Cs^+ occupancy becomes as low as 30%, whereas above 200 mM the Cs^+ occupancy levels off at approximately 65% and is therefore higher than the expected value of 50% for charge neutrality. Both limits thus show unexpected behavior, and in order to explain both of these limits, the standard surface complexation model must be extended.

3.2.1. Low salinity limit: H^+ adsorption

For the lowest salinity values measured, the coverage converges to approximately 35%, which is 15% smaller than the expected 50%. This suggests that the muscovite-electrolyte interface carries a net surface charge equivalent to approximately 15% of the total number of adsorption sites. A unit cell of muscovite has an area of 0.47 nm^2, which, since the system as a whole must be charge neutral, would imply that a net surface charge of -0.64 e/nm^2 has to be compensated by a charge in the electric double layer. However, this is an order of magnitude higher than the net surface charge measured by AFM [11], shown in Fig. 4b as a function of salinity. Additionally, such high surface charges do not agree with previous SFA [3,4], AFM [10] and zeta potential [37,44,45] measurements for muscovite mica at a pH value close to 6.

Additional positive charge in the Stern layer is thus required for a net surface charge that is compatible with literature. Cs^+ adsorption mainly takes place in an inner-sphere configuration in the muscovite cavity site, as was also observed in the current work [16,28]. Outer-sphere Cs^+ is thus not expected to give a large con-

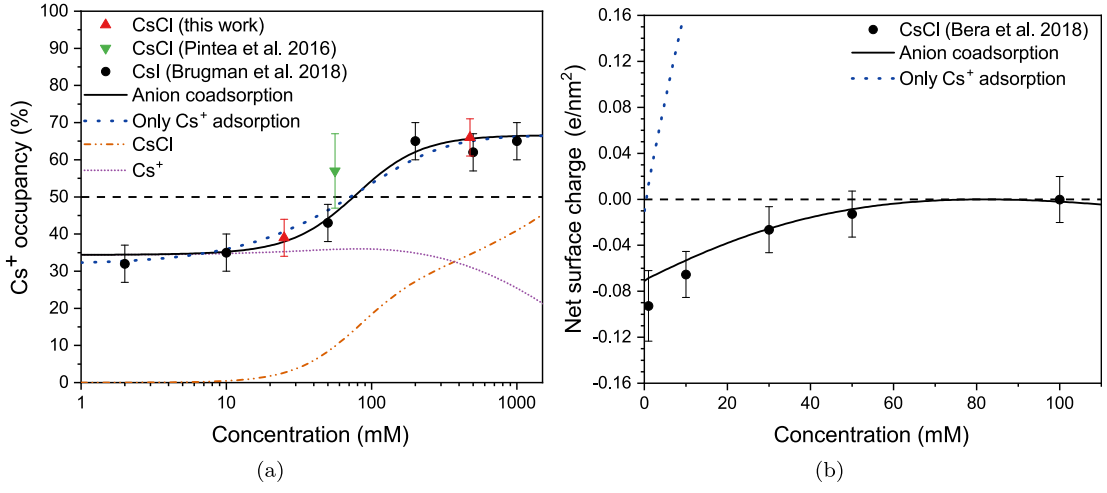

Fig. 4. (a) Occupancy of adsorbed inner-sphere Cs^+ at the basal muscovite surface at room temperature as a function of the CsCl or CsI concentration [18,19]. The dashed line at 50% indicates the occupancy of Cs^+ required to compensate the muscovite negative surface charge. The other lines indicate the occupancy of both Cs^+ (purple dotted) and CsCl (orange dot-dashed) species following from the best adsorption model fit and Cs^+ occupancy (blue dotted) if no Cl^- coadsorption is taken into account. (b) Net surface charge as measured using AFM by Bera et al. [11]. The dashed line indicates a neutral net surface charge. The solid black lines in both (a) and (b) shows the best fit of the chloride coadsorption model with an intrinsic surface charge of $36 \pm 1\%$, $pK_{Cs} = 1.2 \pm 0.3$ and $pK_{CsCl} = 0.7 \pm 0.2$. (For interpretation of the references to colour in this figure legend, the reader is referred to the web version of this article.)

tribution in positive charge. There are no other cations present in solution, except for hydronium. We therefore investigated the possible adsorption of H_3O^+ [19]. The concentration of H_3O^+ is in the order of μM, [19], which means that the affinity of H_3O^+ to muscovite should be high, which was observed before [3,4,46,47]. To investigate possible H_3O^+ adsorption we adopt a Cs^+/H^+ competition model, as has been used previously [3,44,47,48]. Typically, it is assumed that adsorption only takes place at half of the total adsorption sites (one per unit cell). We have adjusted this model in order to be able to account for coverages exceeding 50%. In the Cs^+/H^+ competition model, H^+ would outcompete and fully replace Cs^+ at low salinity, with the inverse happening at high salinity. This, however, is not corroborated by the data in Fig. 4a, which shows that Cs^+ occupancy saturates to a non-zero value for decreasing salinity. The data suggests, therefore, that Cs^+ does not compete with a different cation at low salinities; if it did, the coverage would decrease more strongly as the salinity decreases. Note that at very low salinities ($\ll$2 mM) the Cs^+ occupancy must eventually converge to zero. The best fit of the Cs^+/H^+-competition model is found to be unsatisfactory, even if a Stern layer capacitance is included (see the Supporting Information (S1.2)). Based on the data presented in this article we conclude that the Cs^+/H^+-competition model is not appropriate to describe the muscovite-electrolyte interface under our experimental conditions.

The shortcomings of the Cs^+/H^+ competition model have been noted before in the case of muscovite mica [49,50] and silica [51]. Nevertheless, this conclusion is unexpected, as previous studies clearly show that the zeta potential and net surface charge of muscovite mica do depend on the pH of the solution [10,37,44,50,52]. Here we should note, however, that the same experiments show that in the presence of 1 mM of salt, the zeta potential of muscovite is relatively independent of pH for pH > 6, suggesting that at these pH values the protons are (almost) entirely outcompeted by the cations. Furthermore, this assertion agrees with the surprisingly small value of pK_H found previously [50,52].

If there is no Cs^+/H^+ competition, the low Cs^+ coverage at low salinity must have a different origin. Previous studies have already emphasized that protons behave differently from other cations concerning competitive adsorption on a wide variety of surfaces [53]. For example, a hysteresis of the coverage with pH was observed in the case of muscovite [47], and it was suggested that muscovite mica undergoes an irreversible reaction with protons which penetrate into the lattice and decrease the intrinsic surface charge of muscovite mica. A different study found similar effects for calcinated mica [52], whereas others showed that the cation/proton adsorption models cannot capture the pH dependence of muscovite mica and suggested that oxonium ions behave fundamentally different than the other cations [49]. If protons indeed penetrate the muscovite lattice irreversibly and alter the intrinsic surface charge when muscovite is brought in contact with an aqueous solution, this could explain why in our case the Cs^+ occupancy levels off to approximately 35% instead of a value closer to 50% as expected beforehand. This would mean that the preparation of the muscovite samples is of great importance to the cation adsorption. In order to incorporate this in our surface complexation model, which can only describe reversible adsorption processes, we consider the intrinsic surface charge of muscovite, $-e\sigma_{int}$, as a fit parameter.

3.2.2. High coverage limit: anion coadsorption

The high-salinity saturation value of approximately 65% shows that Cs^+ adsorbs in a structure in which approximately every 2 out of 3 adsorption sites are covered. However, from basic adsorption mechanics one would expect the coverage to saturate at 100% for high salinities. The Cs^+ coverage can only level off at a value lower than 100% if there is a process that prohibits Cs^+ from adsorbing on every adsorption site. A honeycomb lattice where an unoccupied site is surrounded by 6 occupied sites, would be a plausible configuration: to fill this unoccupied site, a Cs^+ ion would need to break the hydration shell and overcome the high electrostatic repulsion of the surrounding six adsorbed ions at the expense of a significant (free-) energy penalty. In order to incorporate the observed maximum coverage into the model, we assign a larger area of occupation to the cations than the area of an adsorption site, as was first proposed by Pashley [3]. This effectively reduces the maximum coverage below unity. See the Supporting Information (S1.1) for more details.

Actually, there is another issue with the high salinity occupancy. The Cs^+ occupancies of 65% at high salinity suggest an unusually large positive surface charge. The overcompensation of 15% over the intrinsic surface charge of 50% (which is an even larger overcompensation if we adjust the intrinsic surface charge to a lower value as argued above) would result in a an unusually high, positive surface charge. Most importantly, however, the variation in the Cs^+ occupancy as measured by SXRD (see Fig. 4a) is not at all comparable to the variations in the net surface charge (see Fig. 4b). This implies that the variations observed in the Cs^+ coverage are largely charge neutral variations. An additional, negative contribution to the total surface charge is therefore required, especially at large salinities. The most obvious candidate is the coadsorption of Cl^-, as was already suggested by previous studies for Cs^+ [29], Rb^+ [54] and K^+ [55], although for the latter two this was only observed for higher salinities than considered in our study. The site density of muscovite is approximately 4 sites per nm^2, so a coverage of 33% corresponds to a local concentration at the surface exceeding 4 M within the Stern layer (assuming for simplicity a thickness of 0.5 nm). Considering the Cs^+ coverage values, even at low salinities, the formation of cation-anion complexes is thus quite plausible. Previous SXRD measurements have, on the other hand, found no evidence of (structured) anion adsorption. [19,38]. However, SXRD can only exclude ordered anion coadsorption, whereas a more disordered structure would still be possible. Such a disordered structure is plausible since the cavities are already filled by the Cs^+ ions, and as a result the Cl^- adsorbed on top is expected to be distributed more homogeneously as it is laterally less confined. [56]. At the expense of a third fit parameter (pK_{CsCl}) we can include this coadsorption process in the model. This parameter is related to a (free) energy gain for the Cl^- ion to be close to the adsorbed Cs^+, which, similar to cation adsorption, can likely be related to the reorganisation of the hydration shell of Cl^-. A surface complexation model cannot, however, explain where this (free) energy gain originates from, only that it must exist.

Here we will only consider Cl^- as the coadsorbing anion, as it is the most abundant anion. The only other anions present are OH^- and HCO_3^- (the CO_3^{2-} concentration is negligible close to pH = 6), which, contrary to Cl^-, do not vary with the salinity and therefore give different predictions. However, as mentioned above, the surface charge of muscovite mica has been shown to be relatively independent of pH for pH>6, making it unlikely that either OH^- and HCO_3^- (or even CO_3^{2-}) have a significant effect on the muscovite mica - electrolyte interface. See Supporting Information (S1.3) for an analysis of such a model.

The chloride coadsorption model (black solid lines Fig. 4) is able to simultaneously fit the Cs^+ occupancies and the net surface charge, as can be seen from the solid lines in Fig. 4. The best fit was obtained with an intrinsic surface charge $\sigma_{int}/\Gamma = 0.36 \pm 0.01$, $pK_{Cs} = 1.2 \pm 0.3$ and $pK_{CsCl} = 0.7 \pm 0.2$. Although the pK_{CsCl} value and the intrinsic surface charge cannot be compared to previous studies, the pK_{Cs} value deviates

significantly from previously determined values. However, the values in previous studies were found either by using a Cs^+/H^+ competition model [3,17,47], and/or by ignoring the electrostatic interactions to the adsorption model [17,47]. The pK_{Cs} found here is a direct result of the adapted model which, we should note, is a minimal model needed to explain both the SXRD and the AFM data. If we consider Cs^+ adsorption without coadsorption, we would find $pK_{Cs} = 3.5$ as a best fit (blue dotted line in Fig. 4a), which is much closer to previously reported values [17]. This value is, however, completely incompatible with the net surface charge data [11] (blue dotted line Fig. 4b). In fact, a surface complexation model without an anion coadsorption reaction predicts a (large) positive net surface charge charge for all considered salinities, and is therefore unable to reproduce both data sets. The best fit pK_{Cs} value also deviates significantly from Molecular Dynamic simulations [31]. This discrepancy can possibly be attributed to the different conditions between the Molecular Dynamics simulations and the Langmuir adsorption models, as the former operates in the NpT ensemble and a salt-free environment, while the latter operates in the μVT ensemble and does incorporate the anions.

Even though we have found adequate fits for both data sets, this of course does not mean that the proposed model is a complete description of the muscovite-electrolyte interface. For example, the Cl^- coadsorption model predicts a strongly decreasing net surface charge for salinities exceeding 100 mM due to the increasing Cl^- (co)adsorption. However, we must keep in mind that for salinities exceeding 100 mM the Poisson-Boltzmann theory begins to break down as the Debye length becomes comparable to the ion size. Furthermore, we have implicitly assumed that the Cl^- and I^- coadsorption constants are equal (i.e. $pK_{CsCl} = pK_{CsI}$). This is reasonable, since the CsI and CsCl data are in good agreement. A more complete model would not only take the different coadsorption constants into account, but also the different ionic radii of the two anions via a triple layer model. This would introduce additional fit parameters, more than we can reliably fit with the current data. It is clear, however, that the simplest model that reproduces both the SXRD and surface charge data requires anion coadsorption. This model will be used below to describe the Cs^+/Ca^{2+} competition data.

3.3. Cation competition

Now that the surface structure of muscovite in contact with pure CsCl or $CaCl_2$ solutions has been determined and a surface complexation model is developed, it is possible to look at the cation competition. The difference in electron density between adsorbed Ca^{2+} and Cs^+ is large, therefore the cation occupancies in the presence of both salts can be derived from the observed changes in the crystal truncation rods. This is illustrated by the specular crystal truncation rod in Fig. 5 for a total salt concentration of 25 mM. At a solution composition of 25% Ca^{2+}/ 75% Cs^+ (green in Fig. 5), the specular crystal truncation rod looks similar to that of only Cs^+ (yellow in Fig. 5). As expected, when the Ca^{2+} concentration is further increased the shape of the crystal truncation rod changes towards the shape of 100% Ca^{2+} (blue in Fig. 5). All measured crystal truncation rods were fitted using a similar structural model as described before, in which the simultaneous adsorption of both cations was incorporated.

The adsorption of cations takes place at the same adsorption site as was found for the single salt conditions, i.e. the cavity site. For Cs^+, this is in agreement with literature, as only a small fraction of Cs^+ is reported to adsorb at other adsorption sites [16,28]. As mentioned before, for divalent cations, including Ca^{2+}, multiple adsorption sites were proposed in literature. Besides the partially hydrated cavity site, a partially hydrated adsorption site above the Si/Al atoms and a fully hydrated outer-sphere adsorption site were proposed [28,31,32,33]. In our measurements, however, we observe neither of these alternative Ca^{2+} adsorption sites. This means that these adsorption states are either not present, or, similar to the coadsorbed anions, too disordered to give a measurable signal. If indeed outer-sphere Ca^{2+} is too disordered to observe, this would mean that the total Ca^{2+} occupancy would be higher than reported in Figs. 6 & 7, and consequently the Cl^- coverage would be higher too. For other divalent cations, such as Sr^{2+} and Zn^{2+}, total cation occupancies of 0.64 ± 0.16 and 0.38 ± 0.02 atom/surface unit cell were found at comparable pH values [32,57]. Our inner-sphere Ca^{2+} occupancies of 0.56 ± 0.16 and 0.90 ± 0.16 atom/surface unit cell are already close to or even higher than thanthe total occupancy of the other cations, implying that the outer-sphere Ca^{2+} occupancy should be low for a comparable total occupancy. This is

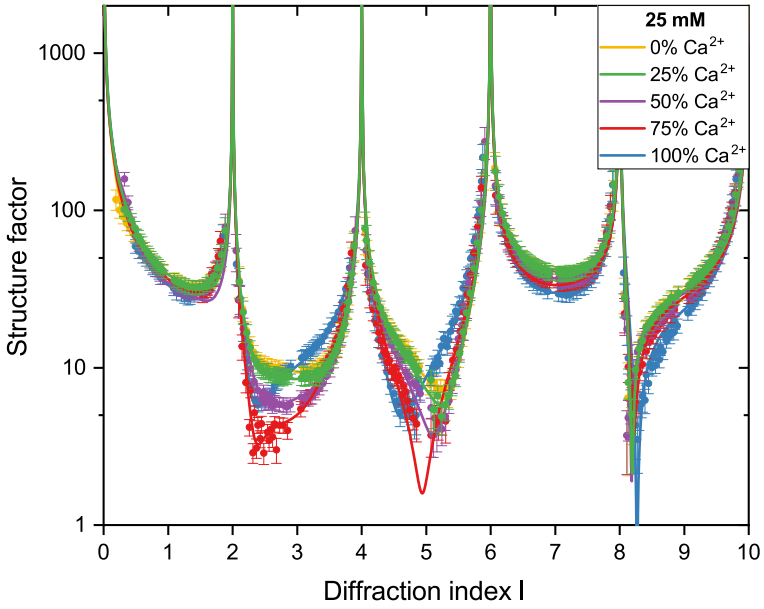

Fig. 5. Specular crystal truncation rod for muscovite in contact with different percentages of Ca^{2+} and Cs^+ at a total salt concentration of 25 mM. The solid lines show the best fit for each crystal truncation rod.

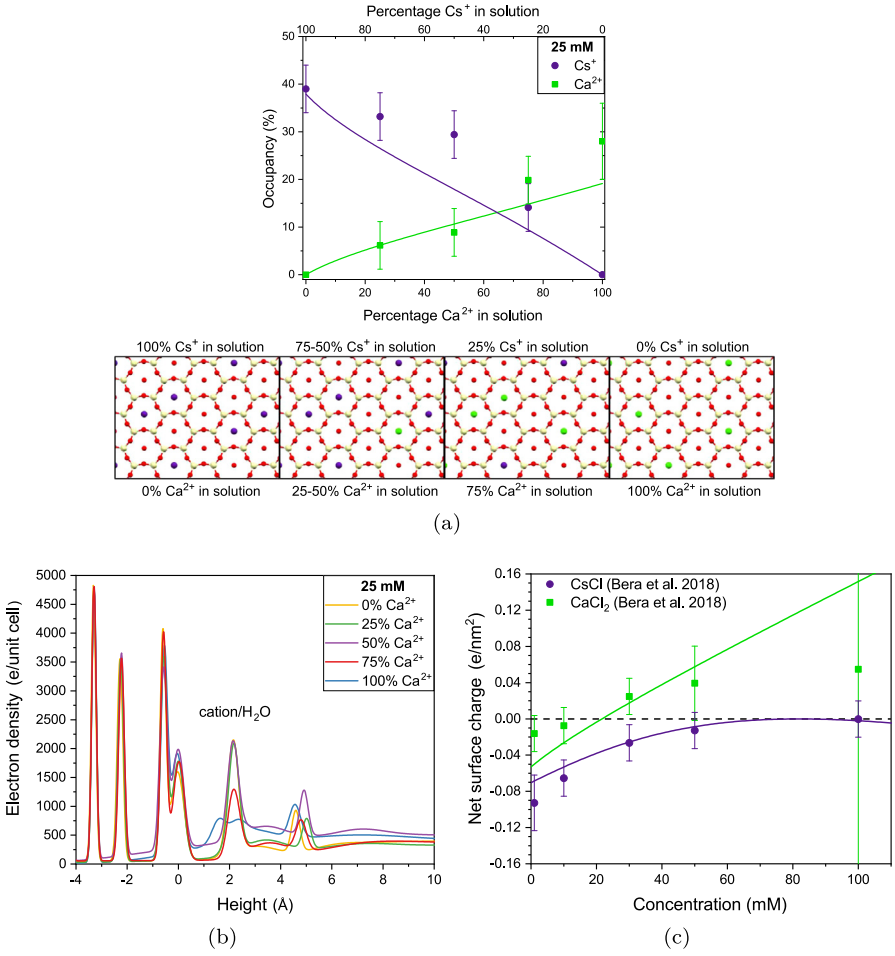

Fig. 6. (a) Upper panel: inner-sphere Ca^{2+} and Cs^{+} occupancies for a total salt concentration of 25 mM at different relative concentrations. Lower panel: Illustration of adsorption of both cations above the center of the hexagonal cavity (Ca^{2+} in green, Cs^{+} in purple and water in red). Note that SXRD is not sensitive to the local adsorption arrangements. (b) Electron density perpendicular to the surface for muscovite in contact with solutions of 25 mM with different Ca^{2+}/Cs^{+} ratios. (c) The associated net surface charge as measured using AFM by Bera et al. [11]. The solid lines in (a) and (c) show the best fit of the Cs^{+}/Ca^{2+} competition model, giving an intrinsic surface charge $\theta_{int} = 36 \pm 1\%$ and reaction constants given by $pK_{Cs} = 1.3 \pm 0.1$, $pK_{CsCl} = 0.7 \pm 0.1$, $pK_{Ca} = 1.0 \pm 0.2$ and $pK_{CaCl} = .0.4 \pm 0.1$. (For interpretation of the references to colour in this figure legend, the reader is referred to the web version of this article.)

in agreement with molecular dynamics simulations, which showed that for Ca^{2+} and other divalent cations inner-sphere adsorption is more favorable than outer-sphere adsorption [31]. The interfacial structure we propose here does not require the extra Ca^{2+} sites and gives a consistent description of SXRD and AFM data. For completeness, the effect of additional outer-sphere Ca^{2+} on the competition results will be discussed in more detail below.

Fig. 6a shows the resulting cation occupancy as a function of solution composition derived from this structural model, for a total salt concentration of 25 mM. At a composition of around 75% Ca^{2+} and 25% Cs^{+}, both cations have similar occupancies, and therefore we can tentatively conclude that Cs^{+} has a higher affinity to the muscovite basal plane than Ca^{2+}. The electron density perpendicular to the surface (Fig. 6b) shows that the muscovite interfacial structure does not significantly change when the cation composition is varied, aside from the electron density at the position of the cations. Also at a total salt concentration of 475 mM, Cs^{+} has a higher affinity to the muscovite basal plane than Ca^{2+}, as both cations have equal occupancies around a solution composition of 80% Ca^{2+} and 20% Cs^{+} (Fig. 7a). Again, the interfacial structure does not change for varying cation compositions except for the cation electron density (Fig. 7b).

Competition experiments were also performed at 63 ± 2 °C for a salt concentration of 475 mM. Whereas the interfacial structure of muscovite in contact with only Ca^{2+} or Cs^{+} remains unaffected at this temperature, differences between room and high temperature conditions are found in the occupancies during cation competition, as shown in Fig. 7. At a solution composition of 75% Ca^{2+} and 25% Cs^{+}, the occupancy of Cs^{+} did not decrease compared to 100% Cs^{+} ($\theta_{Cs^{+}} = 68 \pm 5\%$), whereas for the same composition at room temperature the occupancy had already decreased significantly ($\theta_{Cs^{+}} = 36\% \pm 5\%$). Therefore, Cs^{+} has an even higher affinity to the muscovite surface at high temperature when compared to Ca^{2+}.

As in the case of the Cs^{+} adsorption isotherm, we can set up a surface complexation model to reproduce the cation coverage data measured by SXRD, as well as the net surface charge of pure Cs^{+}-mica and Ca^{2+}-mica measured by Bera et al. using AFM [11]. In the Cs^{+}/Ca^{2+} competition model we also need to include coadsorption of an anion to Ca^{2+}. A minimal model thus includes the following four adsorption reactions,

$$\begin{aligned} S + Cs^{+} &\rightleftharpoons SCs^{+}, \qquad SCs^{+} + Cl^{-} \rightleftharpoons SCsCl, \\ S + Ca^{+} &\rightleftharpoons SCa^{2+}, \qquad SCa^{2+} + Cl^{-} \rightleftharpoons SCaCl^{+}. \end{aligned} \tag{4}$$

Again, Cl^{-} was chosen as the coadsorbing anion. We can then use the surface complexation model to fit both the AFM net surface charge and the SXRD cation coverage data, in order to obtain the four fit parameters pK_{Cs}, pK_{CsCl}, pK_{Ca} and pK_{CaCl}. The result is shown

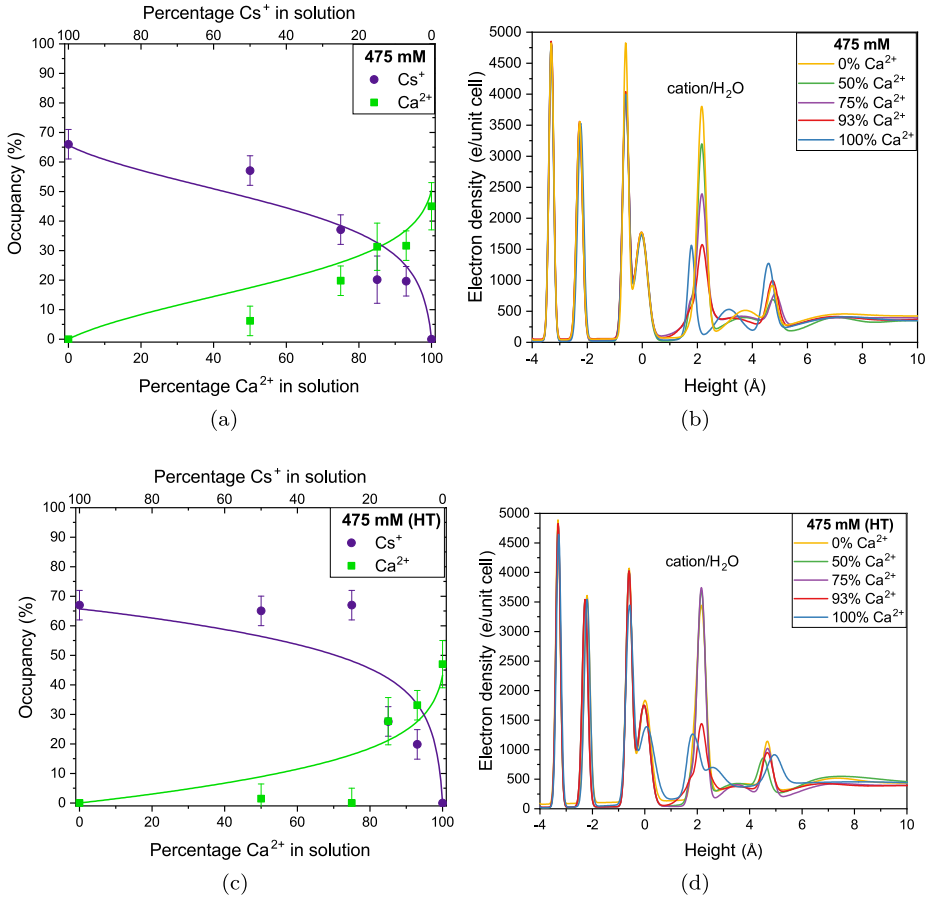

Fig. 7. (a) Measured and fitted inner-sphere Ca^{2+} and Cs^{+} occupancies and (b) electron density perpendicular to the surface for muscovite in contact with different Ca^{2+}/Cs^{+} ratios at a total salt concentration of 475 mM. The solid line in (a) is obtained with the same fit parameters as in Fig. 6. (c) Ca^{2+} and Cs^{+} occupancies and (d) electron density perpendicular to the surface for muscovite in contact with different Ca^{2+}/Cs^{+} ratios at a total salt concentration of 475 mM at a temperature of 63 ± 2 °C. The typical fit shown as the solid lines in (c) is computed with the same fit parameters as in Fig. 6, except here for $pK_{Ca} = 0.4$.

in Figs. 6 and 7. The parameters used for the best fit, which was obtained by fitting all room temperature data, were $pK_{Cs} = 1.3 \pm 0.1$, $pK_{Ca} = 0.9 \pm 0.2$, $pK_{CsCl} = 0.7 \pm 0.1$ and $pK_{CaCl} = 0.4 \pm 0.1$ and with the other parameters the same as used in Fig. 4. The pK_{Ca} value is close to previously reported values [4,48], and can be found using the point of zero charge exhibited by Ca^{2+}-mica around 15 mM.

The surface complexation model can easily be extended to include a possible Ca^{2+} outer-sphere contribution. In this case, the total Ca^{2+} occupancy ($\theta_{Ca^{2+}}$) will consist of $\theta_{Ca^{2+}_{IS}}$ and $\theta_{Ca^{2+}_{OS}}$, where $\theta_{Ca^{2+}_{IS}}$ is reported in Figs. 6 and 7. Within surface complexation models, the ratio between occupancies of different adsorption states of an ion, for example inner and outer-sphere, is independent of the (bulk) density of the ion. If we assume, as an example, that $\theta_{Ca^{2+}_{OS}} = 0.3 \times \theta_{Ca^{2+}_{IS}}$, the model is still capable of reproducing the experimental data. We find that the pK_{Cs} and pK_{CsCl} values are not affected by additional outer-sphere adsorption of Ca^{2+}. As expected, the pK_{Ca} value decreases (becomes 0.6 ± 0.2 in this case), whereas the pK_{CaCl} value increases (becomes 1.0 ± 0.1). This means that the reported pK_{Ca} is possibly overestimated, whereas pK_{CaCl} is underestimated if outer-sphere adsorption of Ca^{2+} occurs. More importantly, our surface complexation model is robust under these conditions and can qualitatively describe general trends observed in the data, such as the higher affinity of Cs^{+} than Ca^{2+} for the muscovite basal plane. A similar analysis holds for, for example, an additional adsorption site above the Si/Al atom. This too is a second adsorption state, since there is not enough room to adsorb both in the cavity and above the Si/Al atom, although we should note that this additional site is not reflected in the SXRD data.

For the high temperature data set, the model has too many parameters to find a unique fit. Since the temperature has changed significantly, we expect all reaction constants to change, but we cannot accurately predict these with the current data. That is not to say, however, that we cannot obtain any information from the HT data. For example, we can fix three reaction constants and fit the fourth one to see if the fit improves compared to the RT values. This will of course not give a unique fit, but does give an indication how a reaction constant is likely to change under the increased temperature. Such an analysis suggests that decreasing pK_{Ca} (fit shown as the solid lines in Fig. 7c) or pK_{CaCl} compared to the other reaction constants improves the fit more than adjusting pK_{Cs} or pK_{CsCl} does. This simple analysis therefore suggests that, although the affinity of both Cs^{+} and Ca^{2+} will most likely decrease, the affinity of Ca^{2+} probably decreases more compared to the affinity of Cs^{+}. This qualitative trend is corroborated by the data in Fig. 7, showing that Ca^{2+} only manages to outcompete Cs^{+} at an even higher Ca^{2+} percentage compared to room temperature.

The uncertainties in the parameters were determined via the covariance matrix associated with the data and the model and by testing the effect of excluding part of the data. We find that the values of the cation adsorption constants, pK_{Cs} and pK_{Ca}, are very robust under such changes (variations less than 0.1 from the best fit values stated above), while the Cl^{-} coadsorption constants, pK_{CsCl} and pK_{CaCl}, are slightly less robust (variations less than 0.5 from the best fit values stated above) depending on the data sets

included in the fitting procedure. Furthermore, we know that the Poisson-Boltzmann theory used to fit the data generally becomes less reliable for salinities exceeding 100 mM, and is therefore less accurate for the measurements at 475 mM.

Instead of focussing on the specific value of the reaction constant, we focus on the results that are independent on the details of the model. One of the most important of such results is that we consistently find that $pK_{Ca} < pK_{Cs}$, i.e. that Ca^{2+} has a lower affinity to the muscovite surface than Cs^+. This point is also clearly derived from the SXRD data shown in Figs. 6 and 7. It thus seems that the valency of the ion does not play the dominant role in determining the affinity of an ion to a surface. However, surface complexation models cannot elaborate on the molecular origin of the value of the reaction constant, so based on the current analysis we can only speculate about this. It was already suggested before that hydration of the ions is a major factor in determining the affinity of the ion to a surface [57,58]. As was mentioned before, the cations adsorb above the cavity, and must therefore lose a significant part of their hydration shell. Consequently, it is less favorable for a strongly hydrated ion, such as Ca^{2+}, to adsorb than for a more weakly hydrated ion such as Cs^+. Furthermore, is has been shown that ions with a larger ionic radius (i.e. unhydrated radius), which are more polarisable than smaller ions, adsorb more readily to surfaces with a low dielectric constant [59]. This interpretation is consistent with the observations at high temperature.

We expect that an increasing temperature will weaken the hydration of ions since the solubility of both salts increases with increasing temperature [60]. This is further corroborated by studies on the residence time of water molecules in the hydration shell of ions, which is thought to be directly related to the hydration strength [61,62]. It was found that for both Cs^+ and Ca^{2+} the hydration strength decreases with temperature [62,63–65], suggesting that both hydration energies, and by extension adsorption free energies, decrease with increasing temperature. Similar behavior under temperature variations was found for Cs^+ on kaolinite [66]. Given that Cs^+ is weakly hydrated at RT, it is plausible that its hydration shell is more easily disrupted than the hydration shell of Ca^{2+}, as the temperature increases. This would decrease the affinity of Ca^{2+} more than that of Cs^+, as observed in the data. Within this light, we can also understand why we find that the anion coadsorbs weaker on Ca^{2+} than on Cs^+, as for this process the hydration structure must be disrupted too. However, the hydration of the cations is not the only factor. The hydration of the surface itself, which depends on the cation coverage, should also have a significant impact on the affinity [57,58]. Other possibly relevant effects include the interfacial dielectric constant [67,68] and the localization of the surface charge. A full analysis of this complex, many-body problem is outside the scope of this article.

A second important conclusion, which has already been discussed, is that an anion coadsorption process is required to fit the data. However, it is also clear that the current model can be further refined. For example, we could include a lateral interaction between the adsorbed ions, introduce a second Cl^- coadsorption reaction on Ca^{2+}, have both OH^- and Cl^- coadsorb, or even introduce a different (reversible) proton (co)adsorption reaction. Interestingly, we can improve the quality of the fit by including a lateral repulsion between the adsorbed Cs^+ ions and the adsorbed Ca^{2+} ions (see the Supporting Information (S1.4) for more details). Adding a second coadsorption reaction, however, did not increase the quality of the fit significantly. This model showed signs of overfitting, and based on the current data we refrain from concluding whether such an additional reaction contributes significantly. Such extensions, however, only further complicate the model and introduce more fit parameters. Given the number of parameters already in the model, we do not apply such extensions in the current analysis. Even though the fit improves by including a lateral interaction between the ions, the model still exhibits the same qualitative behavior as the proposed minimal model.

It is clear, thus, that the muscovite-electrolyte interface shows a greater complexity than is usually assumed. The question remains whether these conclusions are unique to muscovite mica or whether they also apply to other surfaces. For example, the cation/proton competition model is known to be inadequate to describe the charging behavior of silica [51].

4. Conclusion

Surface X-ray diffraction is one of the standard techniques to study ion adsorption on mineral surfaces [16,69]. It is well-documented that the adsorption of monovalent cations on muscovite is mainly determined by hydration energy and the fit of the ion with the surface structure [16,28]. The effect of valency on ion adsorption is less known, but is essential for the understanding of, for example, enhanced oil recovery [1,2]. The interfacial structure as determined with surface X-ray diffraction, gives limited insights in the charge balance at the surface. By combining the cation coverage from these experiments with the net surface from AFM [11] or zeta potential [37] measurements, at the same time knowledge about the structure and electrostatics is obtained.

In this work, SXRD was used to determine the interfacial structure of muscovite in contact with competing salts solutions. First, the interfacial structure of muscovite in contact with solely Cs^+ or Ca^{2+} was determined. A minimal surface complexation model was set up that is able to unite the cation occupancies measured with SXRD and the net surface charge measured by AFM in another study [11]. In order to reproduce the results of both techniques commonly used surface complexation models had to be adjusted. Firstly, the intrinsic negative surface charge of muscovite mica was adjusted from 50% to 36% to account for the low salinity behavior of the Cs^+ occupancy, which might be explained by an irreversible proton adsorption reaction. Secondly, the maximum of available adsorption sites was reduced to 65% of the total sites to capture the high salinity behavior. Thirdly, an anion coadsorption reaction was required to account for the large variation in Cs^+ occupancy that is not reflected in the net surface charge. This model was extended to include Cs^+/Ca^{2+} competition, including an anion coadsorption reaction along with Ca^{2+}. The resulting fits of the equilibrium constants confirmed that the affinity of Cs^+ to muscovite is higher than the affinity of Ca^{2+} to muscovite, which shows that a higher valency does not lead to stronger adsorption. Although there was not enough data to obtain a unique fit at high temperature, the measurements suggest that, compared to room temperature, the affinity difference between Ca^{2+} and Cs^+ is increased, in favor of Cs^+ adsorption.

Our results show that a minimal model even for a single salt muscovite-electrolyte interface includes two rarely included processes, namely (i) a reduced intrinsic surface charge (e.g. due to irreversible proton adsorption) and (ii) anion coadsorption. This emphasizes the point that the muscovite-electrolyte interface is a complex system, and cannot be fully described with a single cation/proton adsorption model. Although such models have been employed before with limited success [3,17,47], the present analysis with data from two different experimental techniques shows that these are merely effective models that do not necessarily reflect the physical environment. Our minimal model shows the rich behavior of solid-water interfaces and we encourage future research to further explore this complexity. We expect that similar processes occur at other solid-water interfaces, such as silica, for which it is also known that such cation/proton competition models are inadequate [51].

Declaration of Competing Interest

The authors declare no conflict of interest.

Acknowledgements

This work is part of the Industrial Partnership Programme Rock-on-a-Chip that is carried out under an agreement between BP Exploration Operating Company Limited and the Netherlands Organisation for Scientific Research (NWO). The experiments were performed on beamline I07 at the Diamond Light Source, Didcot, United Kingdom. We are grateful to Jonathan Rawle for providing assistance in using this beamline. This work is part of the D-ITP consortium, a program of the Netherlands Organisation for Scientific Research (NWO) that is funded by the Dutch Ministry of Education, Culture and Science (OCW). The authors thank Frieder Mugele for providing the AFM data and for helpful discussions. Furthermore the authors would like to thank Wiesiek Szweryn for the development of the high temperature equipment.

Appendix A. Supplementary material

Details regarding the surface complexation model, Cs^+/H^+-competition model, hydroxide coadsorption, lateral interaction between adsorbed ions, measured crystal truncation rods and structural parameters. Supplementary data associated with this article can be found, in the online version, at https://doi.org/10.1016/j.jcis.2019.10.009.

References

[1] T. Austad, A. RezaeiDoust, T. Puntervold, Chemical mechanism of low salinity water flooding in sandstone reservoirs, in: SPE Improved Oil Recovery Symposium, Society of Petroleum Engineers, 2010.
[2] A. Lager, K.J. Webb, C.J.J. Black, M. Singleton, K.S. Sorbie, Low salinity oil recovery-an experimental investigation, Petrophysics 49 (01) (2008).
[3] R.M. Pashley, DLVO and hydration forces between mica surfaces in Li+, Na+, K+, and Cs+ electrolyte solutions: A correlation of double-layer and hydration forces with surface cation exchange properties, J. Colloid Interface Sci. 83 (2) (1981) 531–546.
[4] R.M. Pashley, J.N. Israelachvili, DLVO and hydration forces between mica surfaces in Mg2+, Ca2+, Sr2+, and Ba2+ chloride solutions, J. Colloid Interface Sci. 97 (2) (1984) 446–455.
[5] M. Ricci, P. Spijker, K. Voïtchovsky, Water-induced correlation between single ions imaged at the solid–liquid interface, Nat. Commun. 5 (2014).
[6] S.R. Van Lin, K.K. Grotz, I. Siretanu, N. Schwierz, F. Mugele, Ion-specific and pH-dependent hydration of mica–electrolyte interfaces, Langmuir 35 (17) (2019) 5737–5745.
[7] P. Fenter, C. Park, K.L. Nagy, N.C. Sturchio, Resonant anomalous X-ray reflectivity as a probe of ion adsorption at solid–liquid interfaces, Thin Solid Films 515 (14) (2007) 5654–5659.
[8] S.S. Lee, P. Fenter, K.L. Nagy, N.C. Sturchio, Real-time observation of cation exchange kinetics and dynamics at the muscovite-water interface, Nat. Commun. 8 (2017).
[9] C. Qiu, P.J. Eng, C. Hennig, M. Schmidt, Competitive adsorption of ZrO_2 nanoparticle and alkali cations (Li+–Cs+) on muscovite (001), Langmuir 34 (41) (2018) 12270–12278.
[10] P.G. Hartley, I. Larson, P.J. Scales, Electrokinetic and direct force measurements between silica and mica surfaces in dilute electrolyte solutions, Langmuir 13 (8) (1997) 2207–2214.
[11] B. Bera, N. Kumar, M.H.G. Duits, M.A. Cohen Stuart, F. Mugele, Cationic hofmeister series of wettability alteration in mica-water-alkane systems, Langmuir 34 (45) (2018) 13574–13583.
[12] W. de Poel, S. Pintea, J. Drnec, F. Carla, R. Felici, P. Mulder, J.A.A.W. Elemans, W. J.P. van Enckevort, A.E. Rowan, E. Vlieg, Muscovite mica: Flatter than a pancake, Surf. Sci. 619 (2014) 19–24.
[13] W.L. Bragg, Atomic Structure of Minerals, Cornell University Press, 1937.
[14] G. Gaines Jr., The ion-exchange properties of muscovite mica, J. Phys. Chem. 61 (10) (1957) 1408–1413.
[15] W. de Poel, S.L. Vaessen, J. Drnec, A.H.J. Engwerda, E.R. Townsend, S. Pintea, A.E. F. de Jong, M. Jankowski, F. Carlà, R. Felici, J.A.A.W. Elemans, W.J.P. van Enckevort, A.E. Rowan, E. Vlieg, Metal ion-exchange on the muscovite mica surface, Surf. Sci. 665 (2017) 56–61.
[16] S.S. Lee, P. Fenter, K.L. Nagy, N.C. Sturchio, Monovalent ion adsorption at the muscovite (001)–solution interface: Relationships among ion coverage and speciation, interfacial water structure, and substrate relaxation, Langmuir 28 (23) (2012) 8637–8650.
[17] S.S. Lee, P. Fenter, K.L. Nagy, N.C. Sturchio, Changes in adsorption free energy and speciation during competitive adsorption between monovalent cations at the muscovite (001)-water interface, Geochim. Cosmochim. Acta 123 (2013) 416–426.
[18] S. Pintea, W. de Poel, A.E.F. de Jong, V. Vonk, P. van der Asdonk, J. Drnec, O. Balmes, H. Isern, T. Dufrane, R. Felici, E. Vlieg, Solid-liquid interface structure of muscovite mica in CsCl and RbBr solutions, Langmuir 32 (49) (2016) 12955–12965.
[19] S.J.T. Brugman, E.R. Townsend, M.M.H. Smets, P. Accordini, E. Vlieg, Concentration-dependent adsorption of CsI at the muscovite–electrolyte interface, Langmuir 34 (13) (2018) 3821–3826.
[20] M. Ricci, W. Trewby, C. Cafolla, K. Voïtchovsky, Direct observation of the dynamics of single metal ions at the interface with solids in aqueous solutions, Sci. Rep. 7 (2017) 43234.
[21] E. Vlieg, ROD: a program for surface X-ray crystallography, J. Appl. Crystallogr. 33 (2) (2000) 401–405.
[22] N. Güven, The crystal structures of 2 M1 phengite and 2 M1 muscovite, Z Kristallogr. 134 (1–6) (1971) 196–212.
[23] D.T. Cromer, D.A. Liberman, Anomalous dispersion calculations near to and on the long-wavelength side of an absorption edge, Acta Crystallogr. A 37 (2) (1981) 267–268.
[24] B.L. Henke, E.M. Gullikson, J.C. Davis, X-ray interactions: photoabsorption, scattering, transmission, and reflection at E = 50–30,000 eV, Z = 1–92, At. Data Nucl. Data Tables 54 (2) (1993) 181–342.
[25] E.J.W. Verwey, J.T.G. Overbeek, The Theory of the Stability of Lyophobic Colloids, Dover Publications, Mineola, New York, 1999 (Original work published in 1948)..
[26] R. Hunter, Foundations of Colloid Science, Clarendon Press, Oxford, U.K., 1992.
[27] B.W. Ninham, V.A. Parsegian, Electrostatic potential between surfaces bearing ionizable groups in ionic equilibrium with physiologic saline solution, J. Theor. Biol. 31 (3) (1971) 405–428.
[28] I.C. Bourg, S.S. Lee, P. Fenter, C. Tournassat, Stern layer structure and energetics at mica–water interfaces, J. Phys. Chem. C 121 (17) (2017) 9402–9412.
[29] H. Sakuma, K. Kawamura, Structure and dynamics of water on Li+-, Na+-, K+-, Cs+-, H_3O+-exchanged muscovite surfaces: a molecular dynamics study, Geochim. Cosmochim. Acta 75 (1) (2011) 63–81.
[30] M.L. Schlegel, K.L. Nagy, P. Fenter, L. Cheng, N.C. Sturchio, S.D. Jacobsen, Cation sorption on the muscovite (001) surface in chloride solutions using high-resolution X-ray reflectivity, Geochim. Cosmochim. Acta 70 (14) (2006) 3549–3565.
[31] K. Kobayashi, Y. Liang, S. Murata, T. Matsuoka, S. Takahashi, N. Nishi, T. Sakka, Ion distribution and hydration structure in the stern layer on muscovite surface, Langmuir 33 (15) (2017) 3892–3899.
[32] S.S. Lee, P. Fenter, C. Park, N.C. Sturchio, K.L. Nagy, Hydrated cation speciation at the muscovite (001)- water interface, Langmuir 26 (22) (2010) 16647–16651.
[33] A. Meleshyn, Potential of mean force for Ca2+ at the cleaved mica- water interface, J. Phys. Chem. C 113 (41) (2009) 17604–17607.
[34] S. Adapa, D.R. Swamy, S. Kancharla, S. Pradhan, A. Malani, Role of mono-and divalent surface cations on structure and adsorption behavior of water on mica surface, Langmuir 34 (48) (2018) 14472–14488.
[35] S.-H. Loh, S.P. Jarvis, Visualization of ion distribution at the mica- electrolyte interface, Langmuir 26 (12) (2010) 9176–9178.
[36] S. Pintea, W. de Poel, A.E.F. de Jong, R. Felici, E. Vlieg, Solid-liquid interface structure of muscovite mica in $SrCl_2$ and $BaCl_2$ solutions, Langmuir 34 (14) (2018) 4241–4248.
[37] P.J. Scales, F. Grieser, T.W. Healy, Electrokinetics of the muscovite mica-aqueous solution interface, Langmuir 6 (3) (1990) 582–589.
[38] H. Sakuma, H. Nakao, Y. Yamasaki, K. Kawamura, Structure of electrical double layer at mica/KI solution interface, J. Appl. Sol. Chem. Model. 1 (1) (2012) 1–5.
[39] L. Xu, M. Salmeron, An XPS and scanning polarization force microscopy study of the exchange and mobility of surface ions on mica, Langmuir 14 (20) (1998) 5841–5844.
[40] E. Ferrage, C. Tournassat, E. Rinnert, L. Charlet, B. Lanson, Experimental evidence for Ca-chloride ion pairs in the interlayer of montmorillonite. an XRD profile modeling approach, Clays Clay Miner. 53 (4) (2005) 348–360.
[41] I. Siretanu, D. Ebeling, M.P. Andersson, S.L.S. Stipp, A. Philipse, M.C. Stuart, D. Van Den Ende, F. Mugele, Direct observation of ionic structure at solid-liquid interfaces: a deep look into the Stern layer, Sci. Rep. 4 (2014) 4956.
[42] R.D. Shannon, Revised effective ionic radii and systematic studies of interatomic distances in halides and chalcogenides, Acta Crystallogr. A 32 (5) (1976) 751–767.
[43] Y. Marcus, Ionic radii in aqueous solutions, Chem. Rev. 88 (8) (1988) 1475–1498.
[44] S. Nishimura, H. Tateyama, K. Tsunematsu, K. Jinnai, Zeta potential measurement of muscovite mica basal plane-aqueous solution interface by means of plane interface technique, J. Colloid Interface Sci. 152 (2) (1992) 359–367.
[45] N. Debacher, R. Ottewill, An electrokinetic examination of mica surfaces in aqueous media, Colloids Surf. 65 (1) (1992) 51–59.
[46] R.M. Pashley, Hydration forces between mica surfaces in electrolyte solutions, Adv. Colloid Interface Sci. 16 (1) (1982) 57–62.

[47] C. Park, P.A. Fenter, N.C. Sturchio, K.L. Nagy, Thermodynamics, interfacial structure, and ph hysteresis of Rb+ and Sr2+ adsorption at the muscovite (001)- solution interface, Langmuir 24 (24) (2008) 13993–14004.
[48] P. Kékicheff, S. Marčelja, T.J. Senden, V.E. Shubin, Charge reversal seen in electrical double layer interaction of surfaces immersed in 2:1 calcium electrolyte, J. Chem. Phys. 99 (8) (1993) 6098–6113.
[49] P. Claesson, P. Herder, P. Stenius, J. Eriksson, R. Pashley, An ESCA and AES study of ion-exchange on the basal plane of mica, J. Colloid Interface Sci. 109 (1) (1986) 31–39.
[50] V.E. Shubin, P. Kékicheff, Electrical double layer structure revisited via a surface force apparatus: Mica interfaces in lithium nitrate solutions, J. Colloid Interface Sci. 155 (1) (1993) 108–123.
[51] P.J. Scales, F. Grieser, T.W. Healy, L.R. White, D.Y.C. Chan, Electrokinetics of the silica-solution interface: a flat plate streaming potential study, Langmuir 8 (3) (1992) 965–974.
[52] S. Nishimura, P.J. Scales, H. Tateyama, K. Tsunematsu, T.W. Healy, Cationic modification of muscovite mica: An electrokinetic study, Langmuir 11 (1) (1995) 291–295.
[53] C. Krishnamoorthy, R. Overstreet, Behavior of hydrogen in ion-exchange reactions, Soil Sci. 69 (2) (1950) 87–94.
[54] S. Adapa, A. Malani, Role of hydration energy and co-ions association on monovalent and divalent cations adsorption at mica-aqueous interface, Sci. Rep. 8 (1) (2018) 12198.
[55] D. Martin-Jimenez, E. Chacon, P. Tarazona, R. Garcia, Atomically resolved three-dimensional structures of electrolyte aqueous solutions near a solid surface, Nat. Commun. 7 (2016).
[56] N. Radenović, D. Kaminski, W. van Enckevort, S. Graswinckel, I. Shah, M. in't Veld, R. Algra, E. Vlieg, Stability of the polar {111} NaCl crystal face, J. Chem. Phys. 124 (16) (2006) 164706.
[57] C. Park, P.A. Fenter, K.L. Nagy, N.C. Sturchio, Hydration and distribution of ions at the mica-water interface, Phys. Rev. Lett. 97 (2006) 016101.
[58] U. Sivan, The inevitable accumulation of large ions and neutral molecules near hydrophobic surfaces and small ions near hydrophilic ones, Curr. Opin. Colloid Interface Sci. 22 (2016) 1–7.
[59] Y. Levin, A.P. dos Santos, A. Diehl, Ions at the air-water interface: An end to a hundred-year-old mystery?, Phys. Rev. Lett. 103 (2009) 257802.
[60] W.M. Haynes, CRC Handbook of Chemistry and Physics, Taylor & Francis, 2012.
[61] O.Y. Samoilov, A new approach to the study of hydration of ions in aqueous solutions, Discuss. Faraday Soc. 24 (1957) 141–146, https://doi.org/10.1039/DF9572400141.
[62] Y. Marcus, A simple empirical model describing the thermodynamics of hydration of ions of widely varying charges, sizes, and shapes, Biophys. Chem. 51 (2) (1994) 111–127.
[63] G. Engel, H.G. Hertz, On the negative hydration. a nuclear magnetic relaxation study, Ber. Bunsenges. Phys. Chem. 72 (7) (1968) 808–834, https://doi.org/10.1002/bbpc.19680720713.
[64] H.D.B. Jenkins, Y. Marcus, Viscosity b-coefficients of ions in solution, Chem. Rev. 95 (8) (1995) 2695–2724, https://doi.org/10.1021/cr00040a004.
[65] K. Yoshida, K. Ibuki, M. Ueno, Estimated ionicb-coefficients from nmr measurements in aqueous electrolyte solutions, J. Solution Chem. 25 (5) (1996) 435–453, https://doi.org/10.1007/BF00972991.
[66] Z. Chen, Y. Zhao, X. Xu, C. Liu, L. Yang, Structure and dynamics of cs+ in kaolinite: Insights from molecular dynamics simulations, Comput. Mater. Sci. 171 (2020) 109256.
[67] D.J. Bonthuis, S. Gekle, R.R. Netz, Profile of the static permittivity tensor of water at interfaces: Consequences for capacitance, hydration interaction and ion adsorption, Langmuir 28 (20) (2012) 7679–7694.
[68] D. Ben-Yaakov, D. Andelman, R. Podgornik, D. Harries, Ion-specific hydration effects: Extending the Poisson-Boltzmann theory, Curr. Opin. Colloid Interface Sci. 16 (6) (2011) 542–550.
[69] P. Fenter, N.C. Sturchio, Mineral–water interfacial structures revealed by synchrotron X-ray scattering, Prog. Surf. Sci. 77 (5–8) (2004) 171–258.